Influence of inverted-v-braced system on the stability and strength of multi-story steel frames

http://dx.doi.org/10.1590/0370-44672022760017

Iara Santana Azevedo[1,2]
https://orcid.org/0000-0001-7147-6274
Andréa Regina Dias da Silva[1,3]
https://orcid.org/0000-0001-7841-8077
Ricardo Azoubel da Mota Silveira[1,4]
https://orcid.org/0000-0001-8955-0356

[1]Universidade Federal de Ouro Preto – UFOP, Escola de Minas – Departamento de Engenharia Civil, Ouro Preto – Minas Gerais - Brasil.

E-mails : [2]iarasantanaazevedo@hotmail.com, [3]andreardsilva@ufop.edu.br, [4]ricardo@ufop.edu.br

Abstract

Population growth in urban centers, together with the lack of physical space, has led to the construction of increasingly tall and slender buildings. Multiple-story structures present substantial challenges to civil engineering because they have specific requirements for their design, construction, and use. The increased number of floors leads to more lateral displacements resulting from horizontal actions. Under these conditions, to ensure system stability, structural bracing components are commonly adopted. In addition, along with the use of more resistant materials and new construction techniques, it is necessary to improve the methodologies adopted in the structural analysis to offer professionals in the area the conditions to undertake safer and more economical projects with better speed and efficiency. Thus, in this study, numerical analyses were applied to steel planar reticulated structures to evaluate their stability and strength when inserting bracing systems. The study compared the arrangement of the bars and analyzed the influence of the parameters of the bracing systems, such as the properties of the cross-section and the position of the inverted-V-braced system. The MASTAN2 program was used to perform nonlinear static assessments using reticulated finite elements that considered both geometrical and physical nonlinearities. It was observed that the inverted-V-braced system had a substantial impact on all of the structures that were analyzed, providing increased stiffness and, as a result, significantly reducing the frame's lateral displacement.

Keywords: reticulated frame structures, inverted-V-braced system, numerical analysis, finite element method, physical nonlinearity, geometric nonlinearity, stability.

1. Introduction

Steel structures are increasingly used in civil construction because they are lighter, reach large spans, and facilitate the execution and organization of the construction. In addition, they exhibit high productivity when compared to reinforced concrete structures. Structural steel elements have high ductility, which refers to the ability to undergo large deformations before failure. The steel ductility also favors energy absorption, which is extremely important in structures subjected to seismic excitations (Lui, 1999).

For the design of steel structures to be efficient, economical, and safe, the analysis must portray the members and frame behavior as close to reality as possible. Thus, it is fundamental to consider nonlinear effects when developing structural projects. Such effects are associated with the structure's large displacement and the nonlinear constitutive relationship of the material used in the structural components.

Buildings are composed of the intersection of many structural elements, such as columns, beams, arches, slabs, and bracing systems (Chaves, 2009). Braces are substructures made up of bars that prevent or reduce lateral displacements or vibrations in the structure. Their primary function is to provide stability to the structure when it is affected by strong winds or other powerful lateral forces. Thus, these substructures contribute to the reinforcement of the structure's stability (Azevedo, 2021).

This study will evaluate the behavior of vertical and horizontal bracings, which are used to lock beams and columns, with a focus on the inverted-V-braced system. This article also includes a comparison with other types of bracing, such as the knee brace, which is a type of eccentric bracing, and the diagonal and X types of concentric bracing. According to Smith & Coull (1991)

and Azevedo (2021), the most efficient vertical bracing systems are those whose members form trusses with "total" triangles enclosing the entire structure.

In this context, the objective of this study is to carry out advanced numerical analyses of plane reticulated steel structures to evaluate the influence of some parameters of the bracing systems on the system's global elastic and inelastic stability. The study will also evaluate the properties of the cross-section and the position and arrangement of these additional bars (braced system). The MASTAN2 computational program will be used to perform the numerical analyses (McGuire, Gallagher, and Ziemian, 2014).

2. Nonlinear numerical methodology

A structural system is defined as conservative when the work done by internal and external forces is independent of the path taken by the structure when passing from the initial or reference equilibrium condition to any other configuration. This new configuration must meet the system's compatibility relationships and fundamental boundary criteria to be accepted (Silva, 2009).

It is possible to reach the condition of structural equilibrium by applying the Finite Element Method (FEM), that is, dividing the continuous medium into subdomains that are interconnected through the nodal points where the degrees of freedom to be determined are defined, evaluating the total potential energy, and adding the contributions of each finite element. According to this method, such a condition can be expressed in a generalized way as follows:

$$\mathbf{F}_{int}(\mathbf{U}, \mathbf{P}, \mathbf{G}) \cong \mathbf{F}_{ext} \tag{1}$$

where $\mathbf{F}_{int}$ is the vector of internal forces, which is a nonlinear function of the nodal displacements, **U**, of the internal forces in the members, **P**, and of the effects of material inelasticity, **G** (the gradient vector of the interaction surface); $\mathbf{F}_{ext}$ is the vector of external forces, which can be expressed as the product between the load parameter λ and the reference external force vector, $\mathbf{F}_r$, which defines the direction of the acting external forces ($\mathbf{F}_{ext} = \lambda \mathbf{F}_r$).

For the structural system discretization, a finite element with two nodal points is considered, whose inelastic behavior is restricted to the ends of the element that would simulate the formation of plastic hinges. The deformation of the element at the end of the structural element is constituted only by inelastic rotation. Once the plastic hinge is formed, the internal forces in the cross-section must stay on its plastic resistance surface.

The numerical strategy adopted here to solve Eq. (1) is based on the incremental-iterative approach. Therefore, it is more convenient to rewrite the above equation as follows:

$$^{t}\mathbf{F}_{int} + \sum_{e}\left[\mathbf{k}_{l}^{e} + \mathbf{k}_{g}^{e} + \mathbf{k}_{m}^{e}\right]\Delta\mathbf{u}^{e} \cong {}^{t}\mathbf{F}_{ext} + \Delta\lambda\,\mathbf{F}_{r} \tag{2}$$

where the superscript "t" defines the last system equilibrium configuration; **Δu** is the incremental nodal displacement vector of the element "e"; $\mathbf{K}_l^e$ is the element elastic linear stiffness matrix; $\mathbf{K}_g^e$ is the element's geometric stiffness matrix; $\mathbf{K}_m^e$ is the element's matrix that considers the degradation of material strength; Δλ is the load parameter increment. Note that for the second-order inelastic analysis, both geometric and material nonlinearities are considered to define the equilibrium equation.

The matrices in Eq. (2) can be obtained by applying the principle of virtual work, where the internal energy is a function of the axial strain and rotations of the finite element and the modulus of elasticity. Consequently, we can write:

$$\mathbf{k}_{l}^{e} = \int_{L^e} \mathbf{N}^{T}\,\mathbf{D}\,\mathbf{N}\,dx \tag{3}$$

and

$$\mathbf{k}_{g}^{e} = P\int_{L^e}\left[\mathbf{N}_{u}^{T}\,\mathbf{N}_{u} + \mathbf{N}_{v}^{T}\,\mathbf{N}_{v}\right]dx \tag{4}$$

where L^e is the finite element length, **N** refers to the interpolation functions vector, **D** represents the material constitutive relationship matrix, and P is the axial force acting on the finite element. The interpolation function vectors $\mathbf{N}_u$ and $\mathbf{N}_v$ are associated with the axial and lateral displacements, respectively.

The effect of the degradation of the finite element material in the finite element analyses is considered in the matrix $\mathbf{K}_m^e$ (Eq. 2). Following the Plasticity Theory, it is necessary to include the concept of a yield surface resulting from the applied resultant stress. For the adopted finite element, this yield surface is considered to be a continuous convex flow function between the axial force P and the bending moment M in the element cross-section. Symbolically, this function can be represented as follows:

$$\Phi\left(\frac{P}{P_y}, \frac{M}{M_y}\right) = 1 \tag{5}$$

where P_y and M_y are the yielding axial load and bending moment of the cross-section, respectively. Figure 1 shows the interaction curve of the flow surface function **Φ**. The cross-section is in the elastic regime if the force points are inside the surface, and it is in the plastic regime if the force points are on the surface. Points outside the surface are not admissible.

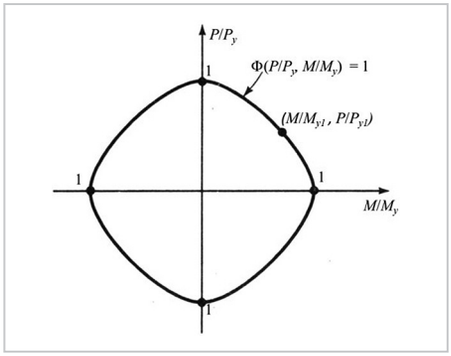

Figure 1 - Cross-section yield surface (Mcguire, Gallagher, and Ziemian, 2014).

The resulting incremental displacement at a yielded finite element node, $\Delta\mathbf{u}$, can be treated as the sum of the elastic contribution, $\Delta\mathbf{u}_e$, and the plastic, $\Delta\mathbf{u}_p$, as presented below:

$$\Delta\mathbf{u} = \Delta\mathbf{u}_e + \Delta\mathbf{u}_p \tag{6}$$

If the normality criterion is considered and applied, we can write:

$$\Delta\mathbf{u}_p = \omega\,\mathbf{G} \tag{7}$$

where $\mathbf{G}$ is the gradient of the interaction surface and ω is the magnitude of the plastic deformation of the analyzed node.

$$\mathbf{G} = \begin{Bmatrix} \dfrac{\partial\Phi}{\partial P} \\ \dfrac{\partial\Phi}{\partial M} \end{Bmatrix} \tag{8}$$

The non-zero components in matrix $\mathbf{G}$ are at the plasticized element nodes. At these points, the axial and flexural stiffnesses reduce. In addition, the elastic deformation contribution is tangent to the yield surface.

The incremental effort vector is derived using the prior relations and considering the orthogonality of the plastic deformations. If ω is arbitrary, it is possible to obtain the finite element plastic reduction matrix, $\mathbf{K}_m^e$, represented by the equation:

$$\mathbf{k}_m^e = -\mathbf{k}_I^e\,\mathbf{G}\left[\mathbf{G}^T\mathbf{k}_I^e\,\mathbf{G}\right]^{-1}\mathbf{G}^T\mathbf{k}_I^e \tag{9}$$

Therefore, the first step in solving Eq. (2) involves evaluating the so-called incremental predicted solution ($\Delta\lambda^0$ and $\Delta\mathbf{u}^0$) for each load step. For this, the initial load parameter increment, $\Delta\lambda^0$, is determined through the strategies available in MASNTAN2, following the determination of the initial displacement increment vector $\Delta\mathbf{u}^0$. However, the predicted solution hardly defines a system equilibrium configuration in a nonlinear structural problem. Thus, the second step involves correcting this predicted solution. These corrections are made using the Newton-Raphson method and continuity numerical techniques to obtain the complete tracing of the equilibrium path. Azevedo (2021) provides more details of the numerical strategy adopted here for solving the nonlinear structural problems.

3. Computational modeling

This section aims to study the effects of the adoption of bracing systems on the stability of structures. For this, static analyses are performed on three different structural systems. As already highlighted, the numerical analyses, which consider the effects of geometric and material nonlinearities, are carried out via the MASTAN2 computer program (McGuire, Gallagher, and Ziemian, 2014).

The first structure examined in the study, a two-story frame, is illustrated in Figure 2, along with the members' properties. The major-inertia direction was considered while modeling the profiles. Vertical loads of variable intensity P were applied at the top of the columns, and horizontal forces of small intensity were used to simulate geometric imperfections. This structure was studied by Chan & Chui (2000) and Silva (2009), who evaluated its load capacity while considering the semi-rigid connections between the beams and the columns.

In order to improve the structural performance, bracing bars arranged in an inverted-V shape were added to the system. The connection of these bars with the other members was articulated. The purpose of the study was to evaluate the influence of the various geometric properties of the sections used in these bars. Three different steel profiles for the locks were used: L89x89x12.5, L76x76x12.5, and L64x64x12.5. The properties of each of them are indicated in Table 1.

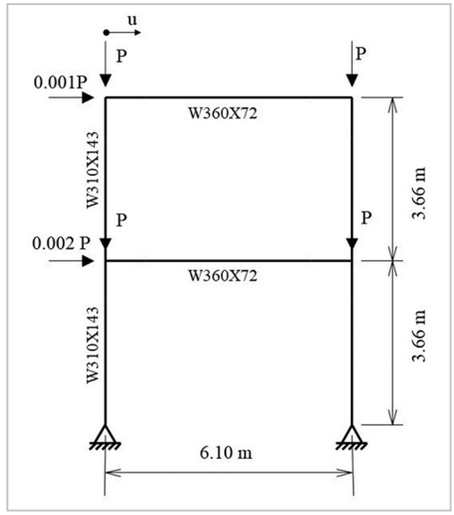

Figure 2 - Two-story steel frame, geometry, and loading.

Table 1 – Properties of the profiles used in bracing.

Profile	Area (cm²)	Inertia (cm⁴)	Plastic module (cm³)
L 64x64x12.5	14.52	51.20	21.14
L 76x76x12.5	17.58	92.40	31.30
L 89x89x12.5	21.00	151.50	43.59

The lateral displacement of the section at the top of the column on the left was regulated for each load intensity during the nonlinear static analysis using the MASTAN2 program, which offers increased structural behavior for each load. The beams and columns were discretized with two and one finite elements, respectively, and the bracing bars were modeled with one element. For the load increment intensity, the maximum number of increments and the maximum load rate applied in the elastic and inelastic analysis were considered, with the values of 10, 10000, and 100000, respectively. The material used had a modulus of elasticity equal to 200000 MPa and a yield strength of 235MPa.

Using the bracing bars with the profile, L89x89x12.5, resulted in the structure becoming more rigid, able to carry a heavier load, and experiencing less displacement, as shown by the elastic analysis (Figure 3(a)). This performance was followed by those rendered using the profiles L76x76x12.5 and L64x64x12.5, respectively. When considering the nonlinear behavior of the material (Fig. 3(b)), regardless of the profile used, the limit load reached was the same — equal to 2160kN — as shown in Table 2. It is worth noting that, for nonlinear effects, the limit load supported by the structure was lower than that considered by the elastic analysis. However, for small load increments at the same load level, the structure suffered less lateral displacement when adopting the L89x89x12.5 profile, followed by the L76x76x12.5 and L64x64x12.5 profiles, respectively. Therefore, it can be concluded that the bracing profile area directly affects the system's stiffness.

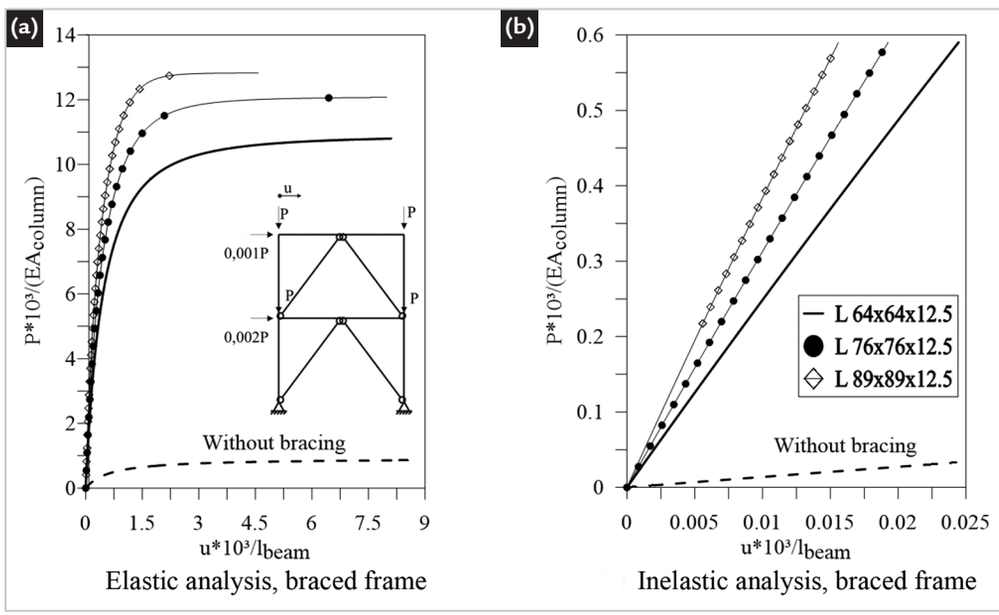

Figure 3 - Two-story steel frame.

Table 2 – Frame limit load with different bracing bars profiles.

Profile	Elastic analysis	Inelastic analysis
L 64x64x12.5	39720 kN	2160 kN
L 76x76x12.5	44080 kN	2160 kN
L 89x89x12.5	46820 kN	2160 kN

The second structure analyzed is the four-story frame presented in Figure 4 Kassimali (1983), Yoo & Choi (2008), and Silva (2009) analyzed this structure to validate nonlinear formulations. The profiles of the beams and columns are also indicated in this figure. The elastic modulus and yield stress were assumed to be 201000 MPa and 236 MPa, respectively.

Referring to the load, as shown in Figure 4, variable vertical loads were applied to the beams at the center of the span and the ends, with the applied force P equal to 133.4 kN. The columns were also subjected to horizontal loads by taking the force as the variable αP. In this study, we set the value of α equal to 0.5. In the analyses, these loads were increased through the parameter λ until the collapse load was reached. For the discretization of the columns and beams, one and two finite elements, respectively, were used. This was consistent with a previous mesh study made by Azevedo (2021). The intensity of the load increment, the maximum number of increments, and the maximum load rate were set to 0.01, 100000 and 100000, respectively, to perform the inelastic analysis.

The effects of different bracing systems were investigated to improve the structural behavior of the frame The bracing was added using diagonally arranged bars, inverted-V and X bracings, and knee bracings, where the bars were positioned with their ends in the middle of the beams and columns. These bars were formed by the L76x76x12.5 profile and articulated with the other members of the structure. The significance of these bracing systems is demonstrated by the equilibrium paths shown in Figure 5, where the displacement of the top of the frame column for the different bracing systems is controlled. It can also be seen that the structure supports a greater load intensity by adopting the arrangement of the bars in an inverted-V.

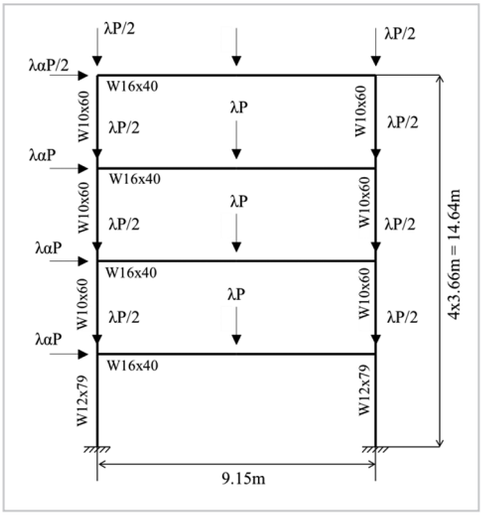

Figure 4 - Four-story steel frame.

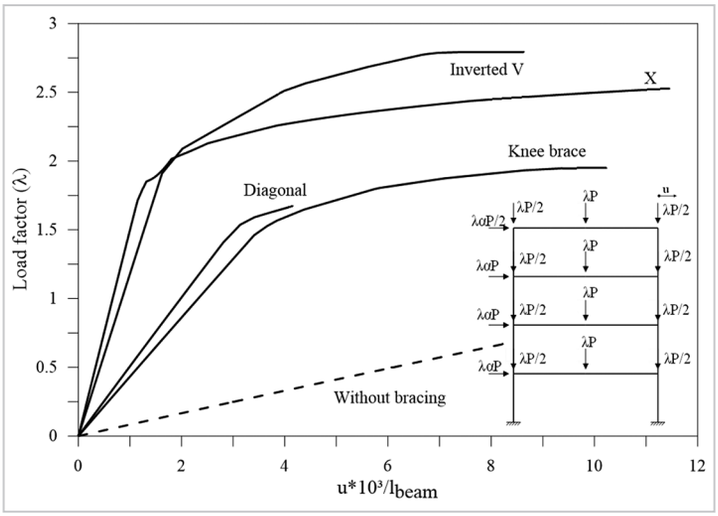

Figure 5 - Comparison between the different bracing systems.

Figure 6 shows the deformed configurations of the structure without bracing, with diagonal bracing, and in inverted-V. Thus, it is evident from Figure 6(a) that hinges occurred more frequently in the beams as axial compression forces increased on these members. Introducing diagonal bracing bars decreased the lateral displacement and produced hinges with a higher load intensity, as shown in Figure 6(b). However, the occurrence sites remained predominantly in the horizontally arranged structural members. In contrast, when bars were inserted in an inverted-V position, only four hinges were located in the beams (Figure 6(c)). It is important to note that the frame collapsed with the formation of plastic hinges in the beams or columns, not with the hinges formed in the bracing bars.

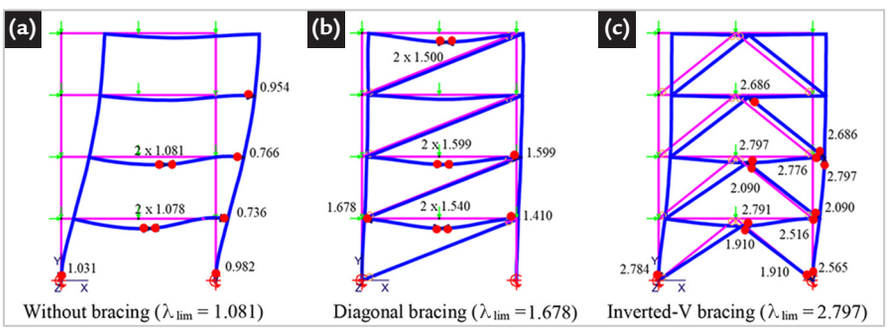

Figure 6 - Deformed configurations of the four-story steel frame.

Finally, Figure 7 illustrates the six-story frame, also known as Vogel's double frame, which was evaluated in the study (Vogel, 1985). In the evaluation, an initial imperfection (a slight slope of the columns) was considered, as shown in Figure 7(a). It also displays the profiles of the beams and columns. The material adopted had a modulus of elasticity equal to 205000 MPa and a yield strength of 235 MPa. The load submitted to the structure is shown in Figure 7(b).

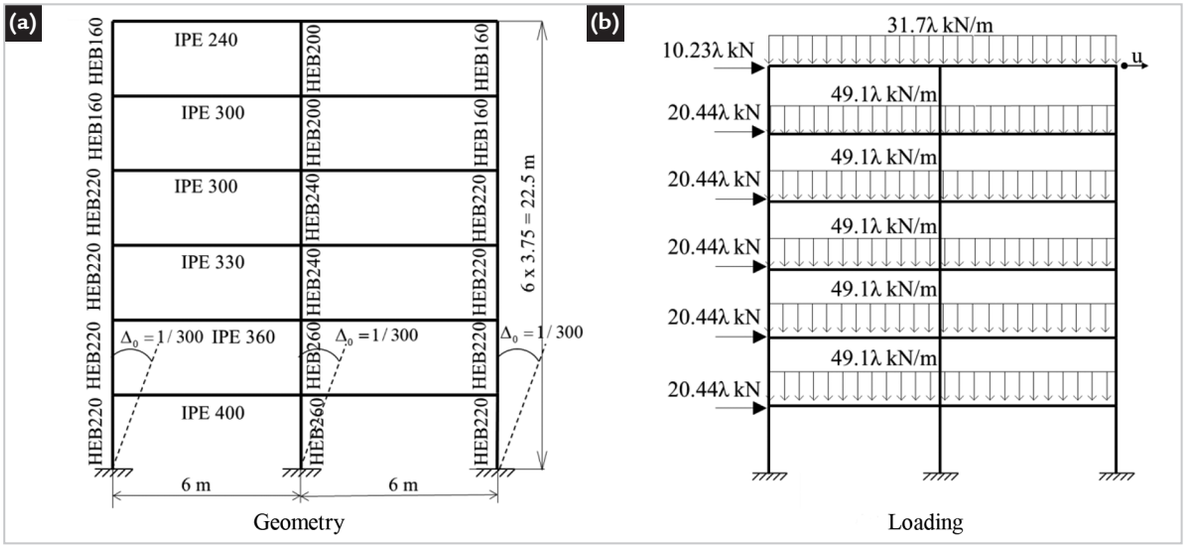

Figure 7 – Six-story steel frame, geometry and loading.

Through inelastic analysis, the effects of the position of bracing systems on the response were investigated. Bars arranged in an inverted-V were then introduced and articulated with the other members. The bars were made of the L76x76x12.5 steel profile and placed in five different positions, as shown in Figure 8. The frame was discretized in each span of the beams, columns, and bracings with seven, two, and one finite elements, respectively. The values of the intensity of the load increment, the maximum number of increments, and the maximum applied load rate were considered to be 0.01, 100000 and 100000, respectively.

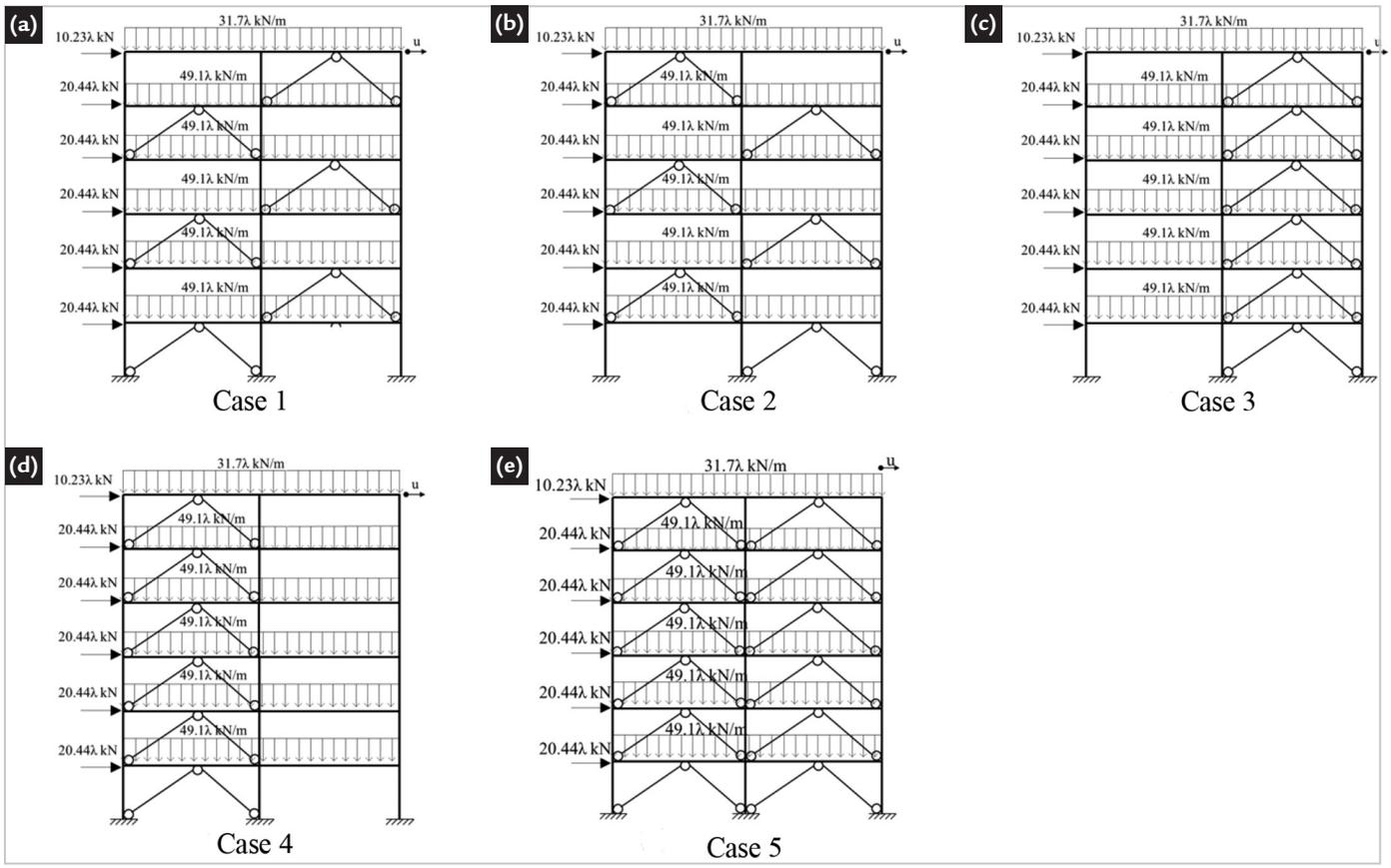

Figure 8 – Characteristics of the bracing system in the six-story steel frame.

Analyzing the equilibrium paths shown in Fig. 9 reveals that all the adopted configurations considerably reduced the lateral displacement of the structure. It is worth noting that, depending on the load to which the

structure will be subjected, arranging the bracing systems only in the left spans (Case 4) may facilitate a more optimized and cost-effective behavior than the one using the provisions of Cases 1, 2, 3, and 5. It is observed that the bars arranged as in Case 4 prevent the top of the frame from experiencing further lateral displacement.

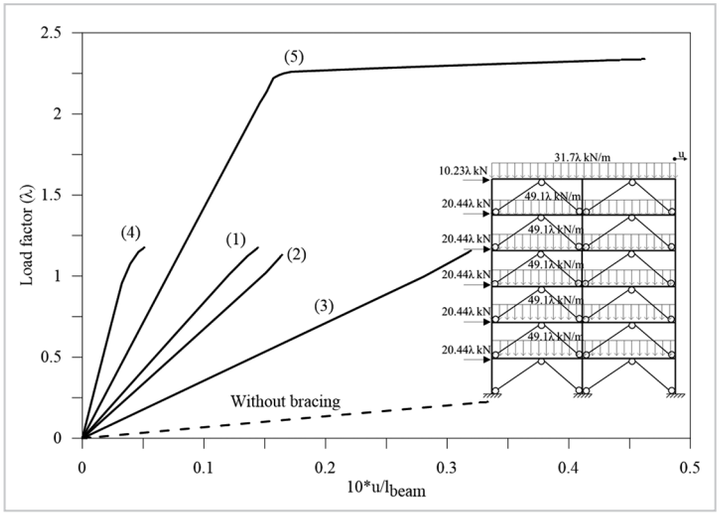

Figure 9 - Inelastic analysis for the six-story braced steel frame.

4. Final comments

Through an analysis of the double-story frame, this study demonstrated that the stiffness of a structural system is affected by the bracing profile area. The lateral displacement of the structure was significantly reduced for the same load level when considering the effects of geometric and material nonlinearities. On the other hand, the load capacity increased significantly only in the elastic analysis. The study also showed how the material's nonlinearity affected the frame response, leading to a significant reduction in the load capacity of the structure when compared to that obtained when considering the elastic material.

Braces were introduced through bars arranged diagonally (in knee bracing, inverted-V, and X) on a four-story structure to study the different bracing systems used in the market. When performing the second-order inelastic analyses, the lateral displacement decreased, regardless of the arrangement of the bars. The majority of the arrangements, however, resulted in a significant increase in the structure's limit load, with the inverted-V position being the most effective. The brace in this position managed to reduce the lateral displacement that destabilized the structure by providing a support point in the center of the beams—places that suffered larger deformations when there was no brace. This brace system contributed to reducing the formation of plastic hinges, thus, providing greater stiffness to the structural system.

During the study of the six-story structure, its second-order inelastic response was verified using an inverted-V-braced system with different arrangements. All the adopted configurations reduced the lateral displacement suffered by the frame. Thus, the importance of choosing a safe, optimized, and cost-effective arrangement was demonstrated for the given requirement.

Acknowledgments

The authors thank CNPq (Conselho Nacional de Desenvolvimento Científico e Tecnológico), CAPES (Coordenação de Aperfeiçoamento de Pessoal de Nível Superior), FAPEMIG (Fundação de Amparo à Pesquisa do Estado de Minas Gerais), PROPEC/UFOP, and PROPPI/UFOP for their support in the development of this research. The authors also extend their gratitude to Professor Ronald Ziemian of Bucknell University for providing the computer program used in this work online.

References

AZEVEDO, I. S. ***Influência do contraventamento na estabilidade e resistência de estruturas em aço.*** 2021. Dissertação (Mestrado em Engenharia Civil) - Universidade Federal de Ouro Preto - Departamento de Engenharia Civil, Ouro Preto, MG, 2021.

CHAN, S. L. CHUI, P. .P. T. ***Non-linear static and cyclic analysis of steel frames with semi-rigid connections.*** Oxford: Elsevier, 2000.

CHAVES, J. R. F. ***Análise dinâmica de pórticos metálicos contraventados.*** 2009. Dissertação (Mestrado em Engenharia Civil e Ambiental - Universidade de Brasília, Brasília, DF, Brasil.

LUI, E. M. Structural steel design. *In:* ***Structural engineering handbook.*** Ed. W.F. Chen, CRC Press LLC, 1999.

KASSIMALI, A. Large deformation analysis of elastic-plastic frames. ***Journal of Structural Engineering,*** v. 109, n. 8, p. 1869-1886, 1983.

McGUIRE, W., GALLAGHER, R. H., ZIEMIAN, R. D. ***Matrix structural analysis.*** 2. ed. Copyright by Ronald D.

Ziemian. 2014.

SILVA, A. R. D. ***Sistema computacional para análise avançada estática e dinâmica de estruturas metálicas.*** 2009. Tese (Doutorado em Engenharia Civil) - Universidade Federal de Ouro Preto - Departamento de Engenharia Civil. Ouro Preto, MG, 2009.

SMITH, B. S., COUL, A. ***Tall building structure: analysis and design.*** New York: John Wiley & Sons, 1991.

VOGEL, U. Calibrating frames**.** ***Stahlbau,*** v. 54, p. 295-31, 1981.

YOO, H., CHOI, D-H., 2008. New method of inelastic buckling analysis for steel frames. ***Journal of Constructional Steel Research,*** v. 64, p. 1152-1164, 2008.

Received: 16 March 2022 - Accepted: 20 October 2022.

CC BY All content of the journal, except where identified, is licensed under a Creative Commons attribution-type BY.